31st Annual International Conference of the IEEE EMBS
Minneapolis, Minnesota, USA, September 2-6, 2009

Preliminary Optimization of Non-Destructive High Intensity Focused Ultrasound Exposures for Hyperthermia Applications

Shutao Wang, Victor Frenkel, Vesna Zderic

Abstract--**Due to its high degree of accuracy and non-invasive implementation, pulsed-high intensity focused ultrasound (HIFU) is a promising modality for hyperthermia applications as adjuvant therapy for cancer treatment. However, the relatively small focal region of the HIFU beam could result in prohibitively long treatment times for large targets requiring multiple exposures. In this work, finite element analysis modeling was used to simulate focused ultrasound propagation and the consequent induction of hyperthermia. The accuracy of the simulations was first validated with thermocouple measurements in hydrogel phantoms. More advanced simulations of *in vivo* applications using single HIFU exposures were then done incorporating complex, multi-layered tissue composition and variable perfusion for an *in vivo* murine xenograft tumor model. The results of this study describe the development of a preliminary methodology for optimizing spatial application of hyperthermia, through the evaluation of different HIFU exposures. These types of simulations, and their validations *in vivo*, may help minimize treatment durations for pulsed-HIFU induced hyperthermia and facilitate the translation of these exposures into the clinic.**

I. Introduction

Mild hyperthermia (HT) is defined as increasing temperatures in the range of 40-45 °C, and may be used as an adjuvant therapy in clinical applications, especially for the treatment of tumors [1]. HT can enhance the sensitivity of tumor cells to radiotherapy [2], and also improve the extravasation of liposomes, where here the effect is on the tumor vasculature [3]. Local HT treatments may be carried out using a variety of methods, including radiofrequency (RF) or microwave applicators [4]. Although presently being used in the clinic for tumor ablation, these techniques suffer from a number of disadvantages including non-uniform heating, and the fact that they are invasive.

High intensity focused ultrasound (HIFU) is presently being used to ablate a number of tumor types in the clinic. The most important advantage of HIFU exposures is that the energy can be provided safely and non-invasively to deep tissue targets using various image guidance modalities, such as diagnostic ultrasound and magnetic resonance imaging [5]. Whereas ablative exposures are provided in continuous mode to enable temperatures to be reached for inducing coagulative necrosis, pulsed exposures can lower rates of energy deposition, so that HT may be achieved non-destructively [6]. Preclinical studies using HIFU for HT have shown how these targeted exposures can deploy drugs locally when used with systemically administered heat sensitive drug carriers [7], as well as control the expression of genes, both temporally and spatially, when the genes possess heat shock protein (HSP) promoters [8]. The inherent disadvantage of the tightly focused HIFU beams is that the volume of treatment is relatively small compared to RF and microwaves. As a result, multiple exposures may be required to 'paint' an entire target, which ultimately could make treatments prohibitively long for clinical application. Optimization of these types of exposures therefore becomes paramount.

To date, studies specifically reporting on simulations of HIFU induced hyperthermia generation have been limited. Examples include predictions of relatively small temperature elevations (e.g. 0.1-0.2 °C) associated with very low rates of energy deposition (i.e using μs pulses and duty cycles of about 15%) for acoustic radiation force imaging (ARFI) [9]. Conversely, simulations for continuous (1-10 s) exposures generating temperature elevations (> 56 °C) required for tissue necrosis have also been carried out [10-12]. In our current study, finite element analysis was used to predict the spatial temperature elevations in tissue resulting from non-destructive pulsed-HIFU exposures at a single treatment spot, where the goal was to optimize heating in the range of 40-44 °C, being ideal for HT applications. A variety of ultrasound exposure parameters were evaluated and direct measurements were performed to validate the predictions. Complex multi-tissue structures were used to represent the *in vivo* environment, including tissue specific perfusion rates.

II. Materials and Methods

A. Simulations

Our simulations were performed using a commercially available finite element software package (SpectralFlex, Weidlinger Associates Inc). SpectralFlex is a numerical program for simulations of long distance acoustic wave propagation in tissues. Similar to a Finite Element method, SpectralFlex is based on the Pseudospectral method, which uses Fourier transforms to calculate the spatial derivatives, ensuring zero dispersion errors at any propagation distance,

Shutao Wang, BSEE is with the Department of Electrical and Computer Engineering, The George Washington University, Washington, DC 20052 USA (email: kevinwst@gwmail.gwu.edu)

Victor Frenkel, PhD is with the Department of Radiology and Imaging Sciences, Clinical Center, National Institutes of Health, Bethesda, MD, 20892 USA (email: vfrenkel@cc.nih.gov)

Vesna Zderic, PhD is with the Department of Electrical and Computer Engineering, The George Washington University, Washington, DC 20052 USA (e-mail: zderic@gwu.edu).

and requires a mesh density of only 2 elements per wavelength, the Nyquist limit [13]. A 4th order time integrator ensures accuracy in the time domain, and allows for all the advantages of time domain calculations including non-linearity, frequency dependant attenuation, and fine control of drive signals. A simple and standard setup for simulating the HIFU exposures appears in Figure 1, including a HIFU transducer, a degassed water bath as a coupling medium, and a uniform target, which in this case is a tissue-mimicking phantom. The material properties used the simulations are listed in Table 1. The attenuation coefficient of the phantom was determined in-house, as described below.

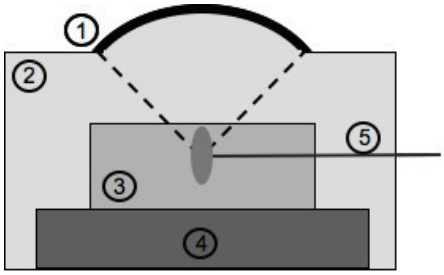

Fig. 1. A schematic of the experimental set up for the simulations and measuring temperature elevations. 1 - HIFU transducer; 2 - degassed water; 3 – phantom; 4 – acoustic absorber; 5 – thermocouple.

B. Tissue-mimicking phantoms

Polyacrylamide-BSA tissue-mimicking phantoms were fabricated as described in Lafon et al [14]. Their key component is bovine serum albumin (BSA), which enhances the acoustic attenuation of the phantom, and enables the generation of heat, where attenuation is proportional to the concentration of the BSA. At lower concentrations (e.g. 7%), the phantom remains relatively translucent, allowing the formation of lesions to be optically visualized. However, as concentration is increased to levels as high as 30%, which renders the attenuation similar to that of soft tissue, the phantoms become completely opaque. As described below, studies with phantoms were carried out in order to validate the simulations. It was important that the phantoms remain translucent in order for the thermocouples to be visible for their accurate placement. Therefore, a BSA concentration of 9% was used when making the phantoms. Although the lower attenuation produced comparatively low temperature elevations by the HIFU exposures (compared to the same exposures in soft tissues), it still enabled reproducible temperatures for validating the simulations. The resulting attenuation of the phantoms was determined using a transmitting and receiving transducer, set in front and behind the phantom, respectively. Ten cycles of 1 MHz sine wave were generated by the function generator to drive the plan wave transmitting transducer (10mm diameter), and the attenuation coefficient, α_c (Np/cm) was calculated as:

$$\alpha_c = \ln \frac{V^*}{V} / d_c + \alpha_w \qquad (1)$$

where d_c is the length of ultrasound pathway in the phantom in cm, V^* is the amplitude of output signal, V is the amplitude of input signal, and α_w is the attenuation coefficient of water in Np/cm.

C. Validation of the Simulations

In order to validate the accuracy of the simulations, they were compared to measurements taken from exposures carried out in the phantoms. A HIFU transducer (TIPS, Phillips Research), which works at 1MHz was used for these experiments [15]. The natural focus of the HIFU transducer is 80 mm, as is the diameter of the transducer. A con-focal window (diameter = 33.5 mm) is present at the center of the transducer for potentially inserting an ultrasound imaging probe. A T-type bare wire thermocouple (TC), 178 μm in diameter (Physitemp, NJ), was connected directly to the TIPS console to measure temperature elevations generated by the exposures. The TC was positioned within the phantom by first inserting it into an 18 G hypodermic needle tip. The two, combined, were then inserted into the phantom, after which the needle tip was retracted, leaving the TC inside. Placement of the needle and TC was done while the phantom was in a degassed water bath (24 °C) to prevent the inclusion of air during the process. The same water bath was used for coupling between the transducer and the phantom. An acoustic absorber was placed under the phantom to prevent reflections of the incident wave. A schematic of the setup appears in Figure 1.

HIFU exposures for these experiments were as follows, and were based on our previous studies of HT applications [7, 16]: total acoustic power (TAP) = 20 W (measured using radiation force balance method); pulse repetition frequency (PRF) = 1 Hz; duty cycle (dc) = 10% (100 ms ON/900 ms OFF); total treatment time = 120 seconds. Temperature measurements were taken as previously described [17] with the TC positioned just at the edge of the focal zone. Initial positioning was carried out visually. Calibrated positioning was performed with the 2D stage of the transducer, by employing single pulses while monitoring temperature elevations in real time. Considerations for corrections for temperature artifacts were done according to Hynynen [18]. Recording of temperatures commenced 20 s prior to turning on the HIFU exposures, and ended when temperatures typically decreased by 75% of their peak values. Measurements were repeated five times. Data was stored and processed off line.

D. Advanced simulations for exposures in subcutaneous xenograft tumors

Previous studies using pulsed-HIFU for hyperthermia were carried out in murine xenograft tumors grown subcutaneously in the flanks [7, 16]. It made sense therefore to simulate *in vivo* exposures that could be verified in this familiar model. A schematic diagram of the complex multi-tissue geometry of this model is shown in Figure 2, where the tumors grow between the overlying skin and the flank muscle. To best depict the true manner by which these

tumors grow, they were represented as a hemisphere (diameter = 6 mm) juxtaposed on a rectangle (3mm × 6 mm). A tumor diameter of 6 mm was chosen to be suitable

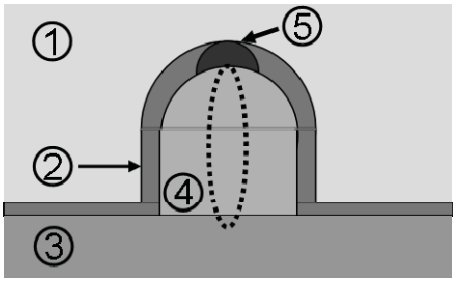

Fig.2 A schematic representation of the subcutaneous xenograft tumors used for the advanced simulations. 1 - degassed water; 2 – skin; (unexposed); 3 – muscle; 4 – tumor; 5 – skin (exposed).

to the dimensions of the focal zone of the transducer. Histological samples have shown that the skin possesses a thickness of approximately 1 mm. Since skin perfusion rate changes dramatically when heated, we created an area in the ultrasound beam path that possessed a 3-fold increase in the normal skin perfusion rate [19]. Both the acoustic and thermal properties of the aforementioned materials can be found in Table 1.

Table 1 – Properties of the materials used in the simulations

	α	c	κ	P
Water	0.0022	4200	0.61	-
Phantom	0.104	4000	0.55	-
Skin*	2.30	3470	0.30	54
Muscle	0.70	3750	0.53	3
Tumor	0.40	3600	0.54	30

where α is the attenuation coefficient in dB/cm, c is the specific heat in J/(kg·K), κ is conductivity in W/(m·K), and P is perfusion rate in kg/(m^3·s).
* value for skin at body temperature. Perfusion rate was increased 3-fold for the exposed skin in the *in vivo* simulations.

The ultrasound transducer used in this simulation is a single element 1MHz focused transducer, having a focal depth of 40 mm and aperture of 50 mm. The axial and radial dimensions of the focal zone (-3dB) were 1.5 and 7 mm, respectively. This device was used previously in the *in vivo* studies discussed above [7, 16]. Because of the sensitivity of the transducer to the build up of heat, an additional requirement for operating the transducer was that duty cycles could not exceed 50%. Simulations were carried out varying the TAP, PRF, and dc. The temperature of the water bath was 36 °C.

III. Results

The attenuation coefficient of the phantom was determined to be $0.0128\pm(7.45\times10^{-4})$ Np/cm at 1 MHz. Based on this value a simulation was generated as depicted in Figure 3, which shows the spatial temperature elevation after a 2 min exposure. The peak temperature was found to be 25.8 °C at the center of the focal zone and 25.2 °C at the radial distance of 1 mm from the center. The mean temperature for the focal zone was 25.6 °C.

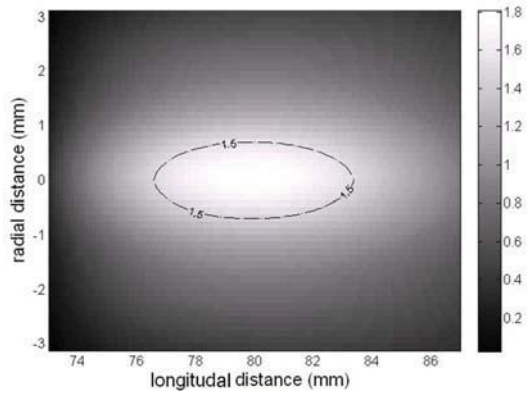

Fig. 3 A simulated pulsed-HIFU exposure, showing the spatial temperature elevation in the focal region after 2 min. The gray scale (on right) is the temperature elevation (°C) and the dotted line indicates the region of active heating in the focal zone. The x-axis originates at the transducer surface.

The average coefficient of variance (CoV = SD/mean) for all the TC measurements over the 2 min exposure was 0.11. Comparison of the simulated and measured temperature elevations showed the mean differential between the two values over the range of measurements taken to be 0.125. Numerous factors could contribute to this difference, such as: variability in the values of diffusivity and attenuation coefficients, errors introduced by thermocouple artifacts, etc. Figure 4 shows the simulated temperature at the edge of the focal zone and the TC measurements taken at the same point.

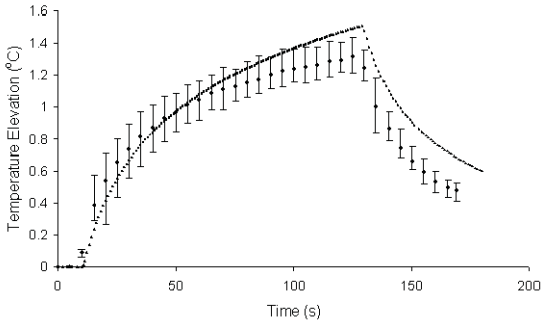

Fig. 4. Comparison of the simulated and measured (n = 5) temperature during a two minute pulsed-HIFU exposure in a phantom. Both simulated and measured temperatures are at the edge of the focal zone (at 1 mm from the center of the focus).

The first set of simulations carried out for the xenograft tumor model compared two exposure parameter sets with equal rates of energy deposition. The first set of exposures that were previously used for *in vivo* studies [7, 16], were done at 20 W, 10% dc, and 1Hz PRF. The second set of exposures utilized 1/5 of the power (i.e. 4 W) and a corresponding 5-fold increase in duty cycle (50%). The PRF also increased 5-fold to 5 Hz, which did not increase the rate of energy deposition. Temperature elevations at the center of the focal zone are seen for each exposure in Figure 5. Whereas the temperature curves appear to be virtually the same for each, the lower power/high duty cycle exposure had a much smoother curve, compared to the relatively large variations in temperature over each cycle for the high

power/low duty cycle exposures. These variations, on average, were 1.6 °C.

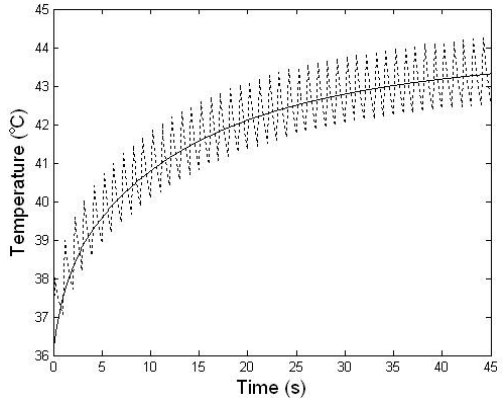

Fig. 5 Comparison of two simulated exposures in the xenograft tumor model. The solid line is for the 4 W; 50% dc; 5 Hz PRF exposures. The dotted line is for the 20 W; 10% dc; 1 Hz PRF exposures. Simulations, at the center of the focus, were carried out until the temperature elevations reached their plateau.

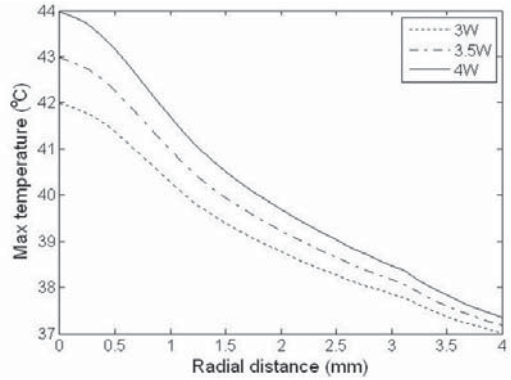

Fig. 6 Simulated peak temperature elevations in the xenograft tumor model as a function of the radial distance from the center of the focal zone. Three different powers (TAP) were evaluated: 3, 3.5, and 4 W. The dc and PRF were constant for all three exposures, being 50% and 5 Hz, respectively.

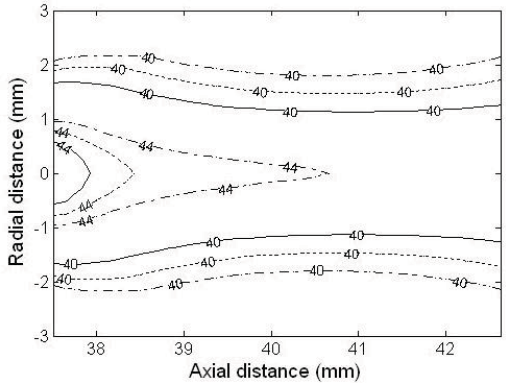

Fig. 7. Spatial distributions of simulated peak temperature elevations in the xenograft tumor model. Three different powers were evaluated: 3 W (solid line), 3.5 W (dotted line), and 4 W (dash dotted line). The dc and prf were constant for all three exposures, being 50% and 5 Hz, respectively. 40 mm is the axial center of the focal zone.

The second set of simulations of *in vivo* exposures looked at the effect of varying the power, while keeping the remainder of the exposure parameters constant, i.e. 50% dc; 5 Hz PRF. As shown in Figure 6, increasing the power from 3 to 3.5 and then to 4 W produced a peak temperature at the center of the focal zone of 42, 43 and 44 °C, respectively. At the radial position of 4 mm from the center, temperatures were approximately the same. Figure 7 depicts the peak spatial distribution for the same 3 exposures (figure 6) of temperatures in the range of 40-44 °C. Calculated as a percentage of the entire tumor area, the area heated within this temperature range was 28.7, 35.0, and 38.6% for the 3, 3.5, and 4 W exposures, respectively.

IV. Discussion

The main objective of this study was to describe some preliminary methodology and results for the optimization of non-destructive, pulsed-HIFU exposures at a single spot for HT applications. The first part of the study involved the validation of relatively simple simulations using measurements in a polyacrylamide-BSA phantom. The second part dealt with increasing the complexity of the simulations for predictions of induced HT in a known preclinical, *in vivo* model that has previously been used with these exposures. To our knowledge studies on simulations of this kind, and their validations, have so far not been reported.

Early on in the design of this study it was decided that validating the accuracy of the simulations would be carried out using phantoms and not in live animals. A number of studies have reported using TCs to measure HIFU induced temperature elevations *in vivo*, both for continuous [18] and pulsed [17] exposures. The associated difficulties for realistic and reproducible results in *in vivo* situations stem from a variety of sources including incorrect placement of the TC, and the heterogeneity of the tissue (e.g. placement of a TC near a large blood vessel, which would record temperature measurements lower than expected). Although the choice of a phantom did not allow for the evaluation of simulations using perfusion, this was not deemed as an overall deficit, seeing that accurate values for perfusion rates of specific tissues are often hard to obtain. Furthermore, the effects of perfusion become even more difficult to predict due to dynamic changes in perfusion in response to active heating. The measurements of HIFU induced temperature elevations in the phantoms were found to be consistent and with a relatively low coefficient of variance. Furthermore, they were observed to be in close agreement with the simulations, providing preliminary justification of the use of the simulations for the second phase of the study involving exposures *in vivo*. An additional advantage of using the phantoms was that we could accurately determine their attenuation coefficient, further increasing the reliability of the simulations. Similar to perfusion rates, accurate data on the acoustic attenuation of biological tissues is also needed; especially for solid tumors where this value can vary greatly from one type to the next.

HIFU exposures used in the first part of the study were previously reported to be effective for significantly enhancing the deployment of drugs from heat sensitive carriers, both in murine tumors [7] and skeletal muscle [16].

Prior investigations of the temperature elevations using pulsed-HIFU exposures showed that these were typically around 4-5 °C [20]. In the second part of the study we looked into modifying these exposures, while keeping the same rate of energy deposition. A decrease in power and corresponding increase in duty cycle showed, along with an increase in pulse repetition frequency (which did not alter the rate of energy deposition), that indeed temperature elevations were the same. In addition, increases were more stable, fluctuating substantially less from cycle to cycle. The decision to reduce the power was in fact based on lowering the mechanical index (MI) of the exposures in order minimize the effects of acoustic cavitation. The 20 W exposures used previously were found to generate both inertial and stable cavitation in murine muscle [17]; however, damaging effects of these exposures were not observed [21]. These results support the use of the same exposures in tumor growth inhibition studies, where compared to untreated controls, tumors treated only with pulsed-HIFU did not have significantly lower growth rates [7]. Despite these results, general considerations for lowering the MI of HIFU exposures are thought to be desirable. In the present study, doing so, with a corresponding increase in duty cycle, was not found to alter the generated heat, and actually produced a more stable hyperthermic treatment. Based on these modified exposures, the subsequent simulations that were performed showed the effect of varying the power in this range for optimizing a hyperthermic range of 40-44 °C.

In conclusion, the present study provided preliminary method development, and results, for optimizing the HIFU exposures for low temperature hyperthermia. Limitations of these results include the fact that simulations involved only single treatment sites and did not describe the potential effects of neighboring treatments, which would modulate both the temporal and spatial heating. However, it is necessary to first accurately describe the effects of single exposures. Furthermore, the effect of active heating on the skin was approximated, where preliminary simulations showed that changes in spatial heating patterns in the proximity of tumor tissue were not unsubstantial when skin perfusion values were varied. These issues and others will be further addressed in our future work. Studies are also being planned to validate the more advanced simulations using therapeutic models for both drug delivery and other applications. An in-depth understanding of the complex interactions between ultrasound energy and biological tissues for HT applications, through a multi-disciplinary approach involving simulations and their validations, will facilitate the optimization of these treatments and expedite their translation to clinic practice.

ACKNOWLEDGEMENTS

We would like to thank Dr. Dieter Haemmerich and Dr. Matthew R. Dreher for valued consultations on the topics of this study. This research was funded, in part, by the intramural research program at the NIH Clinical Center.

REFERENCES

[1] R.W. Habash, R. Bansal, D. Krewski et al., "Thermal therapy, part 1: an introduction to thermal therapy," *Crit Rev Biomed Eng*, vol. 34, (no. 6), pp. 459-89, 2006.

[2] J. Overgaard, "The current and potential role of hyperthermia in radiotherapy," *Int J Radiat Oncol Biol Phys*, vol. 16, (no. 3), pp. 535-49, Mar 1989.

[3] G. Kong and M.W. Dewhirst, "Hyperthermia and liposomes," *Int J Hyperthermia*, vol. 15, (no. 5), pp. 345-70, Sep-Oct 1999.

[4] R.W. Habash, R. Bansal, D. Krewski et al., "Thermal therapy, part 2: hyperthermia techniques," *Crit Rev Biomed Eng*, vol. 34, (no. 6), pp. 491-542, 2006.

[5] J.E. Kennedy, "High-intensity focused ultrasound in the treatment of solid tumours," *Nat Rev Cancer*, vol. 5, (no. 4), pp. 321-7, Apr 2005.

[6] V. Frenkel, "Ultrasound mediated delivery of drugs and genes to solid tumors," *Adv Drug Deliv Rev*, vol. 60, (no. 10), pp. 1193-208, Jun 30 2008.

[7] S. Dromi, V. Frenkel, A. Luk, et al., "Pulsed-high intensity focused ultrasound and low temperature-sensitive liposomes for enhanced targeted drug delivery and antitumor effect," *Clin Cancer Res*, vol. 13, (no. 9), pp. 2722-7, May 1 2007.

[8] R. Deckers, B. Quesson, J. Arsaut, et al., "Image-guided, noninvasive, spatiotemporal control of gene expression," *Proc Natl Acad Sci U S A*, vol. 106, (no. 4), pp. 1175-80, Jan 27 2009.

[9] M.L. Palmeri and K.R. Nightingale, "On the thermal effects associated with radiation force imaging of soft tissue," *IEEE Trans Ultrason Ferroelectr Freq Control*, vol. 51, (no. 5), pp. 551-65, May 2004.

[10] X. Fan and K. Hynynen, "Ultrasound surgery using multiple sonications--treatment time considerations," *Ultrasound Med Biol*, vol. 22, (no. 4), pp. 471-82, 1996.

[11] P.M. Meaney, R.L. Clarke, G.R. ter Haar et al., "A 3-D finite-element model for computation of temperature profiles and regions of thermal damage during focused ultrasound surgery exposures," *Ultrasound Med Biol*, vol. 24, (no. 9), pp. 1489-99, Nov 1998.

[12] F. Chavrier, J.Y. Chapelon, A. Gelet, and D. Cathignol, "Modeling of high-intensity focused ultrasound-induced lesions in the presence of cavitation bubbles," *J Acoust Soc Am*, vol. 108, (no. 1), pp. 432-40, Jul 2000.

[13] B. Fornberg, "A Practical Guide to Pseudospectral Methods," *Cambridge University Press*, 1996.

[14] C. Lafon, V. Zderic, M.L. Noble et al., "Gel phantom for use in high-intensity focused ultrasound dosimetry," *Ultrasound Med Biol*, vol. 31, (no. 10), pp. 1383-9, Oct 2005.

[15] K. Kooiman, M.R. Bohmer, M. Emmer, et al., "Oil-filled polymer microcapsules for ultrasound-mediated delivery of lipophilic drugs," *J Control Release*, vol. 133, (no. 2), pp. 109-18, Jan 19 2009.

[16] P.R. Patel, A. Luk, A. Durrani, et al., "In vitro and in vivo evaluations of increased effective beam width for heat deposition using a split focus high intensity ultrasound (HIFU) transducer," *Int J Hyperthermia*, vol. 24, (no. 7), pp. 537-49, Nov 2008.

[17] B.E. O'Neill, H. Vo, M. Angstadt et al. "Pulsed High Intensity Focused Ultrasound Mediated Nanoparticle Delivery: Mechanisms and Efficacy in Murine Muscle," *Ultrasound Med Biol*, Dec 9 2008.

[18] K. Hynynen, "The threshold for thermally significant cavitation in dog's thigh muscle in vivo," *Ultrasound Med Biol*, vol. 17, (no. 2), pp. 157-69, 1991.

[19] T.R. Gowrishankar, D.A. Stewart, G.T. Martin, et al., "Transport lattice models of heat transport in skin with spatially heterogeneous, temperature-dependent perfusion," *Biomed Eng Online*, vol. 3, (no. 1), pp. 42, Nov 17 2004.

[20] V. Frenkel, A. Etherington, M. Greene, et al., "Delivery of liposomal doxorubicin (Doxil) in a breast cancer tumor model: investigation of potential enhancement by pulsed-high intensity focused ultrasound exposure," *Acad Radiol*, vol. 13, (no. 4), pp. 469-79, Apr 2006.

[21] H.Hancock, L.H. Smith, A. K. Durrani, et al., "Investigations into pulsed-high intensity focused ultrasound enhanced delivery: Preliminary evidence for a novel mechanism," *Ultrasound Med Biol*, in press.